

RESEARCH ARTICLE

# Identification of Elg1 interaction partners and effects on post-replication chromatin re-formation

Vamsi K. Gali<sup>1</sup>, David Dickerson<sup>2</sup>, Yuki Katou<sup>3</sup>, Katsunori Fujiki<sup>3</sup>, Katsuhiko Shirahige<sup>3</sup>, Tom Owen-Hughes<sup>2</sup>, Takashi Kubota<sup>1</sup>, Anne D. Donaldson<sup>1\*</sup>

**1** Institute of Medical Sciences, University of Aberdeen, Foresterhill, Aberdeen, Scotland, United Kingdom, **2** Centre for Gene Regulation and Expression, University of Dundee, Dundee, Scotland, United Kingdom, **3** Research Center for Epigenetic Disease, Institute of Molecular and Cellular Biosciences, University of Tokyo, Tokyo, Japan

\* [a.d.donaldson@abdn.ac.uk](mailto:a.d.donaldson@abdn.ac.uk)



**OPEN ACCESS**

**Citation:** Gali VK, Dickerson D, Katou Y, Fujiki K, Shirahige K, Owen-Hughes T, et al. (2018) Identification of Elg1 interaction partners and effects on post-replication chromatin re-formation. *PLoS Genet* 14(11): e1007783. <https://doi.org/10.1371/journal.pgen.1007783>

**Editor:** Julian E. Sale, MRC Laboratory of Molecular Biology, UNITED KINGDOM

**Received:** June 15, 2018

**Accepted:** October 23, 2018

**Published:** November 12, 2018

**Copyright:** © 2018 Gali et al. This is an open access article distributed under the terms of the [Creative Commons Attribution License](https://creativecommons.org/licenses/by/4.0/), which permits unrestricted use, distribution, and reproduction in any medium, provided the original author and source are credited.

**Data Availability Statement:** All raw-data files for MNase-Seq and ChIP-Seq data are uploaded to Array Express under accession number: E-MTAB-6985.

**Funding:** This work was supported by Biotechnology and Biological Sciences Research Council (BBSRC, <https://bbsrc.ukri.org/>) Grant BB/K006304/1 and Cancer Research UK (<https://www.cancerresearchuk.org/>) Programme Award A19059 to ADD, and Wellcome Trust (<https://wellcome.ac.uk/home>) Grant 095062 to TOH. KS was supported

## Abstract

Elg1, the major subunit of a Replication Factor C-like complex, is critical to ensure genomic stability during DNA replication, and is implicated in controlling chromatin structure. We investigated the consequences of Elg1 loss for the dynamics of chromatin re-formation following DNA replication. Measurement of Okazaki fragment length and the micrococcal nuclease sensitivity of newly replicated DNA revealed a defect in nucleosome organization in the absence of Elg1. Using a proteomic approach to identify Elg1 binding partners, we discovered that Elg1 interacts with Rtt106, a histone chaperone implicated in replication-coupled nucleosome assembly that also regulates transcription. A central role for Elg1 is the unloading of PCNA from chromatin following DNA replication, so we examined the relative importance of Rtt106 and PCNA unloading for chromatin reassembly following DNA replication. We find that the major cause of the chromatin organization defects of an *ELG1* mutant is PCNA retention on DNA following replication, with Rtt106-Elg1 interaction potentially playing a contributory role.

## Author summary

DNA replication is the central process that duplicates the genetic information during cell multiplication. Many cellular factors play important roles in the efficient and accurate duplication of DNA, critical for faithful transmission of genetic information. One such factor is Elg1. Elg1 acts to unload PCNA, the ring-shaped processivity factor that holds DNA polymerases on DNA for replication. In this work, we identify an additional role for Elg1 during replication. We show that lack of Elg1 leads to defects in packaging of DNA into chromatin after DNA replication. In addition, we found that Elg1 interacts with histone chaperones, factors which play key role in chromatin formation. Examining causes of the chromatin re-assembly defect, we show that accumulation of PCNA on DNA is the main cause of defective chromatin formation in the absence of Elg1. By uncovering a new route through which Elg1 ensures chromosomes are perfectly copied, our findings

by Grant-in-Aid for Scientific Research on Priority Areas (15H05970 and 15K21761) from Ministry of Education, Culture, Sports, Science and Technology, Japan. (<http://www.mext.go.jp/en/>). The funders had no role in study design, data collection and analysis, decision to publish, or preparation of the manuscript.

**Competing interests:** The authors have declared that no competing interests exist.

advance understanding of how Elg1 contributes to the stability of the genome through its key roles in DNA replication.

## Introduction

The genetic material in eukaryotes is packaged into chromatin, composed mainly of DNA and nucleosomes. During DNA replication, DNA helicases separate the two parental strands of DNA and nucleosomes are removed from the DNA. Once the nascent DNA strands have been synthesized, the nucleosomal structure must be reassembled to restore the chromatin and permit reinstatement of epigenetic information. Defective chromatin re-assembly leads to improper chromatin formation and loss of epigenetic marks carried on the parental histones, resulting in genomic instability [1].

Various replication-associated factors play a key role in ensuring all the genetic and epigenetic information is efficiently duplicated. A critical component of the replication machinery is PCNA, which serves as the processivity factor for DNA polymerases. Apart from acting as an accessory factor for DNA polymerase, PCNA coordinates replication-associated processes including chromatin re-assembly, cohesion establishment, DNA repair and the damage response [2]. PCNA is loaded onto chromatin during replication by the Replication Factor C (RFC), a pentameric complex consisting of Rfc1-5 [3,4]. During the initiation of each Okazaki fragment, RFC loads PCNA prior to polymerase  $\delta$  recruitment. On completion of each Okazaki fragment, PCNA must then be unloaded, which requires the Elg1 RFC-Like Complex (also called Elg1-RLC; [5,6]. The Elg1-RLC contains the same Rfc2-5 subunits as RFC, but the largest subunit Rfc1 is replaced by Elg1. Timely removal of PCNA is important, and PCNA accumulation in the absence of Elg1 contributes to genomic instability phenotypes such as elongated telomeres, telomeric silencing, chromosomal rearrangements, cohesion defects, and increased sister chromatin recombination [7–11].

Histone chaperones are crucial auxiliary components of the replication machinery [12,13], which ensure the proper coupling of DNA replication with re-assembly into nucleosomes [14]. FACT complex of the budding yeast *S. cerevisiae* contains subunits Spt16 and Pob3, and can bind both H2A-H2B and H3-H4. FACT associates with components of the replication machinery including the MCM complex and DNA polymerase  $\delta$  [15,16] and acts in parental histone recycling and placement on the newly replicated DNA, as well as being implicated in transcription-coupled chromatin control [17,18]. In *S. cerevisiae* newly synthesized histone H3-H4 dimers are bound by the histone chaperone Asf1, with new histone H3 preferentially acetylated at H3K56. Asf1 binding and H3K56Ac modification promote the interaction of new H3-H4 with further histone chaperones including CAF-1 and Rtt106 [19], and Asf1 additionally interacts with RFC [20]. CAF-1 is a three subunit complex consisting in yeast of subunits Cac1, Cac2, and Cac3. Two CAF-1 complexes associate to assemble an H3-H4 tetrasome in the initial step of nucleosome re-assembly [21]. CAF-1 promotes nucleosome assembly at replication forks through interaction with PCNA and by binding to DNA directly [22–24]. Rtt106 is also implicated in nucleosome reassembly following DNA replication. Containing two Pleckstrin Homology Domains that mediate its preference for K56-acetylated H3 [21], Rtt106 has been shown to dimerize to mediate assembly of an H3-H4 tetrasome [25,26]. Deletion of *RTT106* when combined with deletion of *CAC1* showed a defect in deposition of H3K56Ac, which is marker of newly deposited histone in yeast [19,27]. Rtt106 is also involved in heterochromatin formation: *rtt106* $\Delta$  mutant cells exhibit loss of silencing at mating type loci and telomeres [19,28]. In addition, Rtt106 is proposed to be important for nucleosome assembly

during transcription at highly transcribed genes [29] and in regulation of histone gene expression [30,31]. However, it remains unknown how Rtt106 is recruited to required sites of nucleosome assembly.

Because of the links between PCNA and nucleosome assembly, and the effects on chromatin and genome stability caused by *ELG1* deletion [9], we were prompted to investigate whether the PCNA unloading factor Elg1 has a role also in the chromatin re-assembly process. Here we show that Elg1 activity is critical for timely nucleosome organization on nascent DNA. We moreover discovered that Elg1 interacts with histone chaperones, in particular Rtt106 and the FACT complex, with the interaction of Elg1 and Rtt106 not dependent on PCNA. We find however that the most significant cause of defective post-replication nucleosome organization in an *elg1Δ* mutant is delayed unloading of PCNA, with Elg1-Rtt106 interaction potentially playing a contributory role.

## Results

### *In vivo* assays reveal a role for Elg1 in nucleosome assembly

The process of DNA replication and nucleosome re-assembly are tightly coupled. Because it acts at replication forks in PCNA unloading, we examined if Elg1 also affects nucleosome deposition onto newly replicated DNA. Initially, we examined Okazaki fragment length in strains lacking Elg1. Okazaki fragment length can be used as a proxy for nucleosome deposition, since fragment length tends to be determined by the newly deposited nucleosome on the immediately preceding fragment [13,32]. To permit the visualization of Okazaki fragments, we used a strain background with an Auxin-Inducible Degron (AID)-tagged copy of the DNA ligase gene *CDC9*, which accumulates unligated Okazaki fragments during S phase in the presence of auxin. Cells were synchronized in G1 then released into S phase for 55 min, and then Okazaki fragments visualized by 3' end-labelling and gel electrophoresis as described [6,13] (Fig 1A & 1B). In normal cells, Okazaki fragment lengths tend to cluster around 180 bases and 360 bases corresponding to mono- and di-nucleosomal sizes. As previously described, Okazaki fragments are somewhat extended in the mutant *cac2Δ* which lacks the CAF-1 chromatin assembly factor (Fig 1C) [13,32]. This lengthening is believed to reflect aberrant and delayed nucleosome repositioning, which causes continued nick translation and Okazaki fragment lengthening by DNA polymerase  $\delta$ , since it does not encounter a nucleosome on the previously synthesized DNA that would stimulate its disengagement. In an *elg1Δ* mutant, we found that Okazaki fragment lengths also differed from wild-type, showing a generally broader distribution with a higher proportion of fragments extended in length when compared to wild-type (Fig 1C & S1 Fig). This Okazaki fragment lengthening suggests that the *elg1Δ* mutation may cause a nucleosome assembly defect. The lengthened Okazaki fragment phenotype was not shared by a *ctf18Δ* mutant, which lacks the Ctf18-RLC complex that is involved in establishment of cohesion [33,34]. The effect of Elg1 in limiting Okazaki fragment length therefore appears specific to Elg1-RLC. Since Cdc9 depletion is intrinsic to the Okazaki fragment detection assay, we cannot exclude the possibility that lack of Cdc9 contributes to this Okazaki fragment lengthening effect in the *elg1Δ* mutant.

To examine chromatin re-assembly in *elg1Δ* using a different approach, we next tested the sensitivity of chromatin to digestion by Micrococcal Nuclease (MNase), since defective chromatin re-assembly can result in increased accessibility to digestion by this nuclease. There was no evident abnormality in MNase sensitivity of bulk chromatin in an *elg1Δ* mutant. However, defects in replication-coupled chromatin re-assembly tend to be transient and quickly restored following replication by redundantly acting histone chaperones and/or replication-independent histone turnover [35]. To test nucleosome deposition onto newly replicated DNA, we

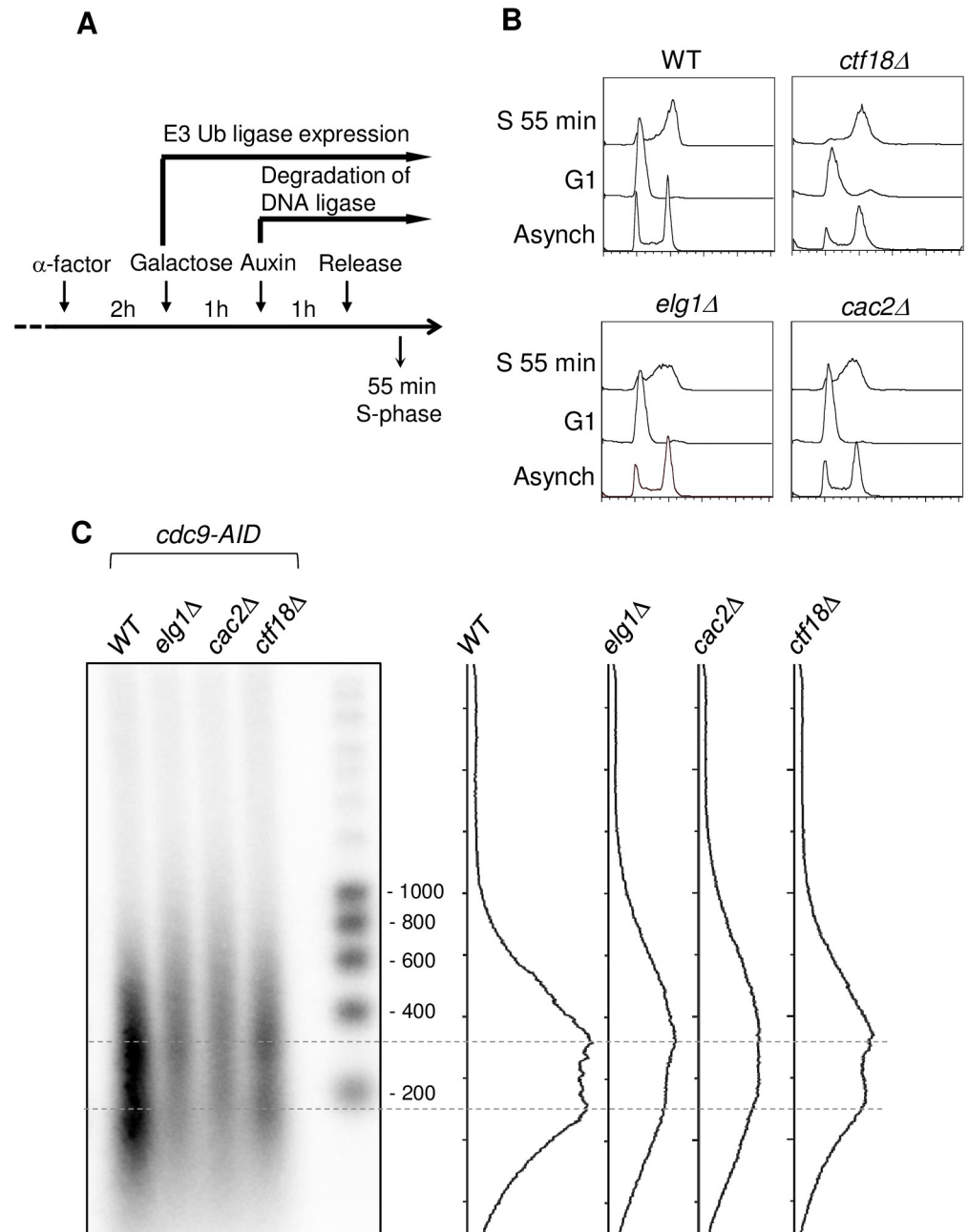


**Fig 1. An *elg1Δ* mutant shows extended Okazaki fragments after DNA ligase depletion, suggesting a nucleosome organization defect.** A. Outline of the experiment for detection of Okazaki fragment length. B. Flow-cytometry profiles of indicated strains showing progression through S phase. C. Autoradiograph of Okazaki fragments in the strains indicated. Okazaki fragments show extended length in *elg1Δ*, similar to *cac2Δ* and unlike *ctf18Δ*. Dotted lines show Okazaki fragments corresponding to mono- and di-nucleosome sizes. Trace of signal intensity for each lane is shown.

<https://doi.org/10.1371/journal.pgen.1007783.g001>

used cultures synchronized by release from  $\alpha$  factor into S phase and examined the MNase sensitivity of nascent DNA labelled with the thymidine analog 5-Bromo 2-deoxyuridine (BrdU) (Fig 2A & 2B). These experiments used strains genetically modified to incorporate BrdU. After Southern blot transfer of MNase-digested DNA to membrane, nascent DNA was

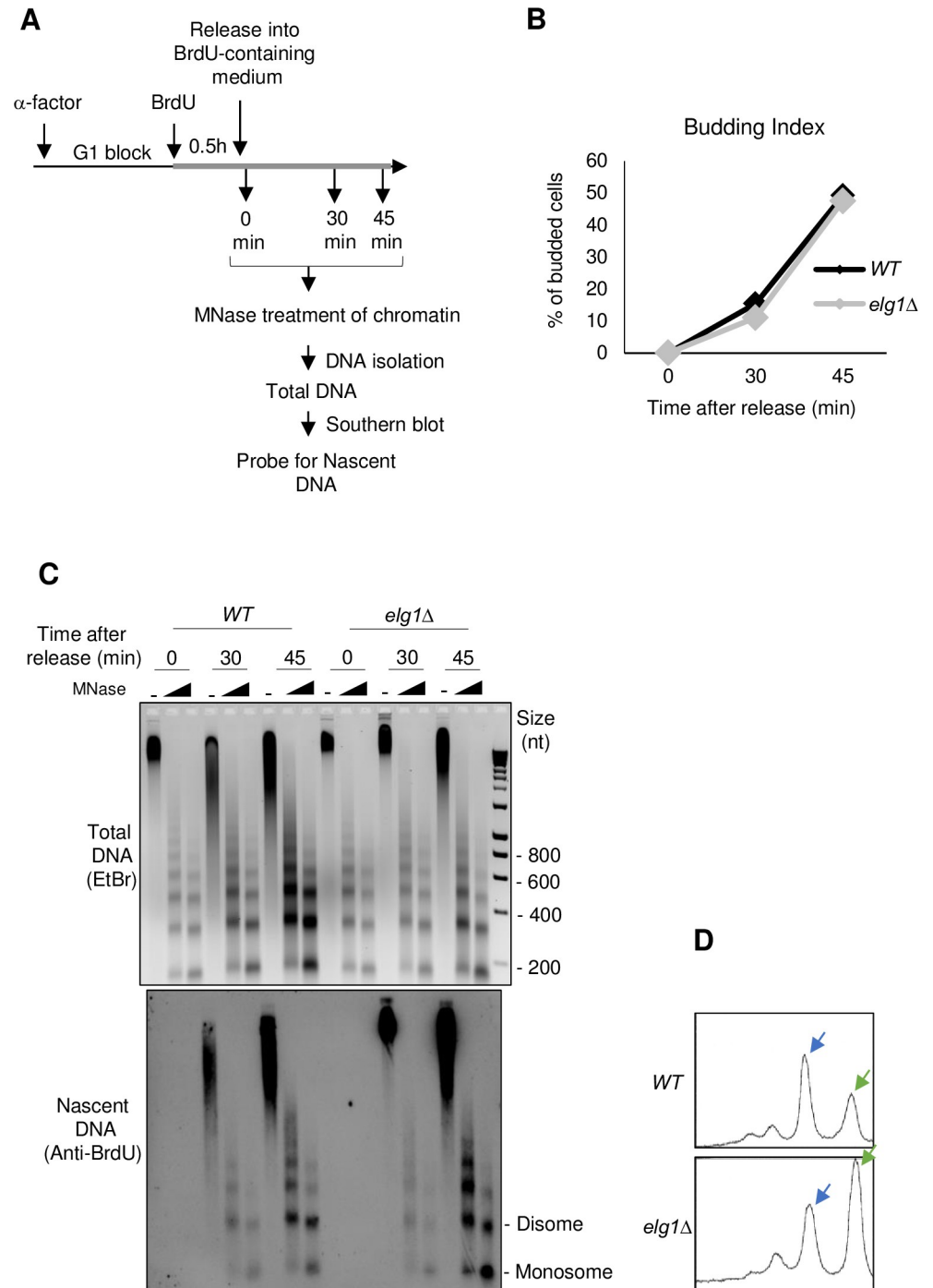


**Fig 2. Sensitivity of nascent chromatin in *elg1Δ* to micrococcal nuclease digestion reveals defective nucleosome assembly.** A. Outline of experiment. Thick grey line indicates the presence of BrdU in the culture medium. B. Budding index (% of budded cells) in WT and *elg1Δ* indicating synchronous progression through S phase. C. Micrococcal nuclease digestion of chromatin from WT and *elg1Δ* strains at indicated times after release into S phase. Upper panel: total DNA on agarose gel detected by Ethidium bromide staining. Lower panel: nascent DNA on membrane probed with anti-BrdU antibody. Micrococcal nuclease (MNase) concentrations: 200 and 600 gel units. D. Signal traces of 45 min, 600 gel units MNase concentration lanes from WT and *elg1Δ*. Blue and green arrows indicate di- and mono-nucleosomal peaks.

<https://doi.org/10.1371/journal.pgen.1007783.g002>

specifically visualized by probing the DNA on the membrane with anti-BrdU antibody. Validating the assay, nascent DNA in a *cac1Δ* mutant (S2C Fig) was more sensitive than wild-type to MNase digestion, due to delayed chromatin re-assembly [35]. We found that nascent DNA in the *elg1Δ* mutant (Fig 2C) was also more sensitive to MNase than wild-type, as evidenced by an increased proportion of mononucleosomal compared to disomal digested fragments (Fig 2C lower panel, compare proportion of disome and monosome bands and signal traces of 45 min samples of nascent DNA in Fig 2D). This increased sensitivity to MNase digestion in *elg1Δ* was reproducible, as illustrated by the additional gels shown in S2A & S2B Fig. The magnitude of the effect did vary between experiments: the proportion of mono-nucleosomal to total nascent DNA was increased 1.7-fold in *elg1Δ* relative to wild-type in Fig 2C, 1.2-fold in S2A Fig, and 2.6-fold in S2B Fig. Such variation is to be expected given the semi-quantitative nature of such experiments, but overall the elevated accessibility of nascent DNA to MNase digestion is indicative of defective or delayed nucleosome assembly. The differences in sensitivity to MNase are not caused by different rates of progression through S phase of WT and *elg1Δ* cells (S3 Fig). To summarize, our observation of extended Okazaki fragments and increased sensitivity to micrococcal nuclease in the *elg1Δ* mutant suggest a role for Elg1 in replication-coupled nucleosome re-organization.

### Genome-wide analysis reveals delayed nucleosome organization during S phase in *elg1Δ*

The results presented above prompted us to investigate effects of the *elg1Δ* mutation on nucleosome assembly genome-wide. We used thymidine analog 5-ethynyl-2'-deoxy-uridine (EdU) to label newly replicated DNA in G1-arrested cells released into S phase. Following MNase digestion, EdU-labelled nascent DNA was isolated by affinity purification (Fig 3A). After deep sequencing [35], nucleosomal reads were then aligned with respect to origins of replication (Fig 3B & 3C) or transcription start sites (TSS) of all genes (S4 Fig). While no difference in the organization of nucleosomes either upstream or downstream of origins was observed in G1 control samples, a clear defect in organization of nucleosomes is observed in *elg1Δ* (Fig 3B) at early time points after release (27 min, 30 min, 33 min) when compared to WT. As cells reach the end of S phase (60 min) the nucleosomal pattern in the *elg1Δ* mutant becomes more organized and similar to WT, consistent with recovery of normal nucleosome distribution as previously described [35]. Defective nucleosome organization in *elg1Δ* mutant is somewhat similar to that seen in a *cac1Δ* mutant (Fig 3C & S4B Fig) although the *cac1Δ* mutant shows an increased spacing of nucleosomes on nascent DNA that is not obviously shared by *elg1Δ*.

### Elg1 interacts with Rtt106 and other histone chaperones

To identify interaction partners of Elg1 potentially connected to nucleosome assembly, we used SILAC-based mass spectrometry to identify co-precipitating proteins. Strains expressing untagged or FLAG-tagged versions of Elg1 were differentially labelled with isotopically light or heavy lysine and arginine, and immunoprecipitated proteins (Fig 4A) were analyzed by mass spectrometry. As expected, the Elg1-FLAG samples showed strong enrichment of Elg1 and Rfc2-5 (the other Elg1-RLC subunits) and also of PCNA. Strikingly, the histone chaperone Rtt106 was also enriched at levels similar to the Rfc2-5 subunits (Fig 4B & 4C). Also enriched were Spt16 and Pob3, two subunits of the FACT complex. Both Rtt106 and FACT complex are implicated in replication-coupled nucleosome assembly: while FACT appears to mediate recycling of parental histones, Rtt106 is involved in depositing newly synthesized histones [18,19,36]. The interactions suggest that these histone chaperones, particularly Rtt106, could potentially mediate the nucleosome assembly role of Elg1.

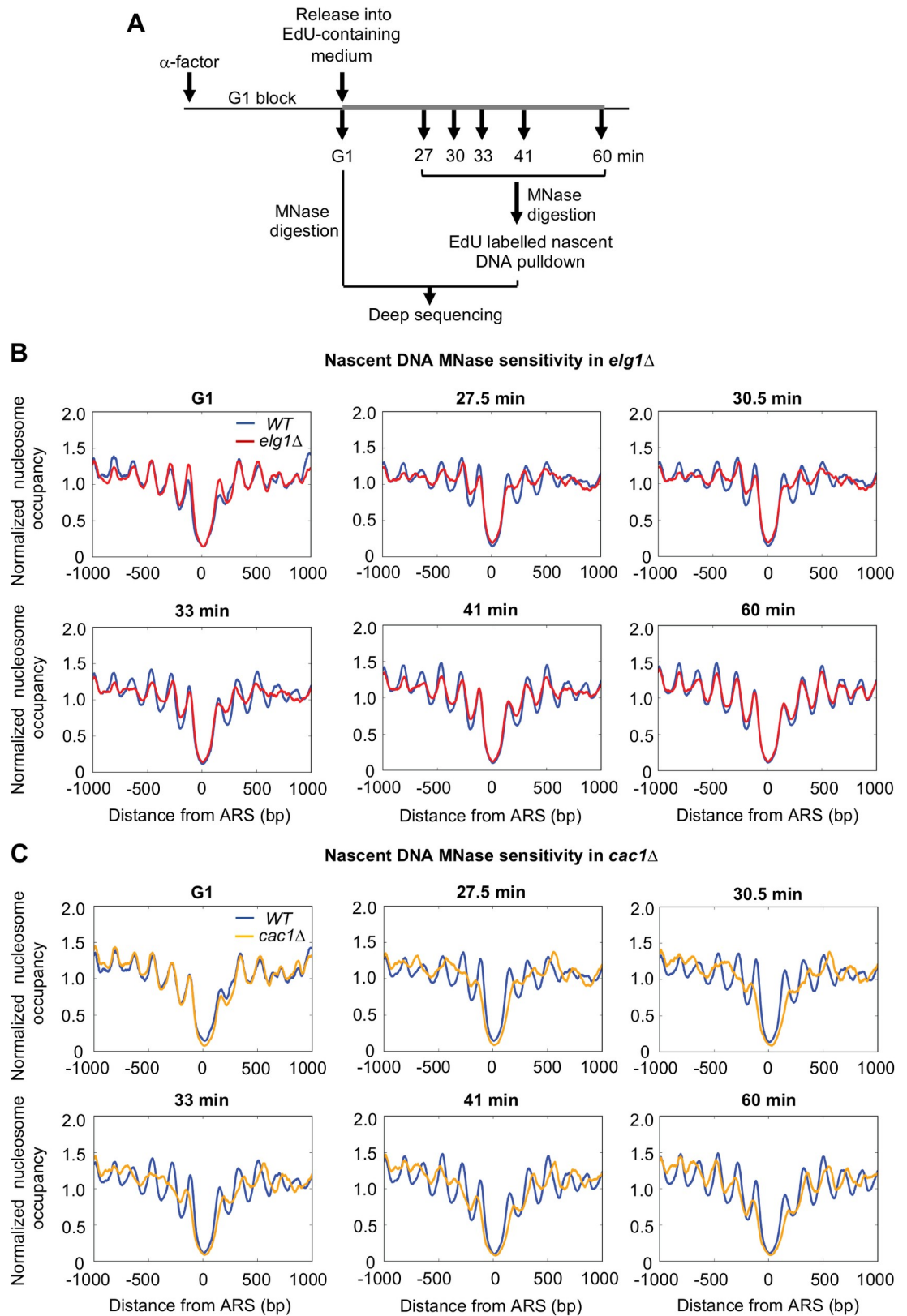


**Fig 3. Genome-wide MNase-seq analysis of EdU labelled nascent DNA shows defective nucleosome organization in *elg1 $\Delta$* .** A. Outline of the MNase-seq experiment. Thick grey line indicates the presence of EdU in culture medium. B & C. Plots showing

protection from MNase of EdU-labelled nascent DNA, aligned to origins of replication (ARS sites) in *elg1Δ* (B) and *cac1Δ* (C) compared to WT. Plots in (B) are mean of two biological replicates shown individually in S5 Fig. G1 samples show MNase-digested total DNA. 27.5–60 min samples show MNase-digested nascent DNA recovered by EdU pull down.

<https://doi.org/10.1371/journal.pgen.1007783.g003>

We carried out further co-immunoprecipitation experiments with Rtt106 to confirm and investigate the Elg1-Rtt106 interaction. Immunoprecipitation of Elg1-FLAG pulled down HA-tagged Rtt106 (Fig 5A). Pulldown of Elg1 truncation mutants showed that both the Elg1 N-terminal and C-terminal regions are important for the interaction with Rtt106 (S6 Fig). These regions are unique to Elg1, having only very limited sequence similarity with Rfc1 or Ctf18. Consistently, neither Rfc1 nor Ctf18 showed interaction with Rtt106 in co-immunoprecipitation experiments (Fig 5B), suggesting interaction with Rtt106 is a property specific for Elg1 amongst the major subunits of RFC and its related complexes.

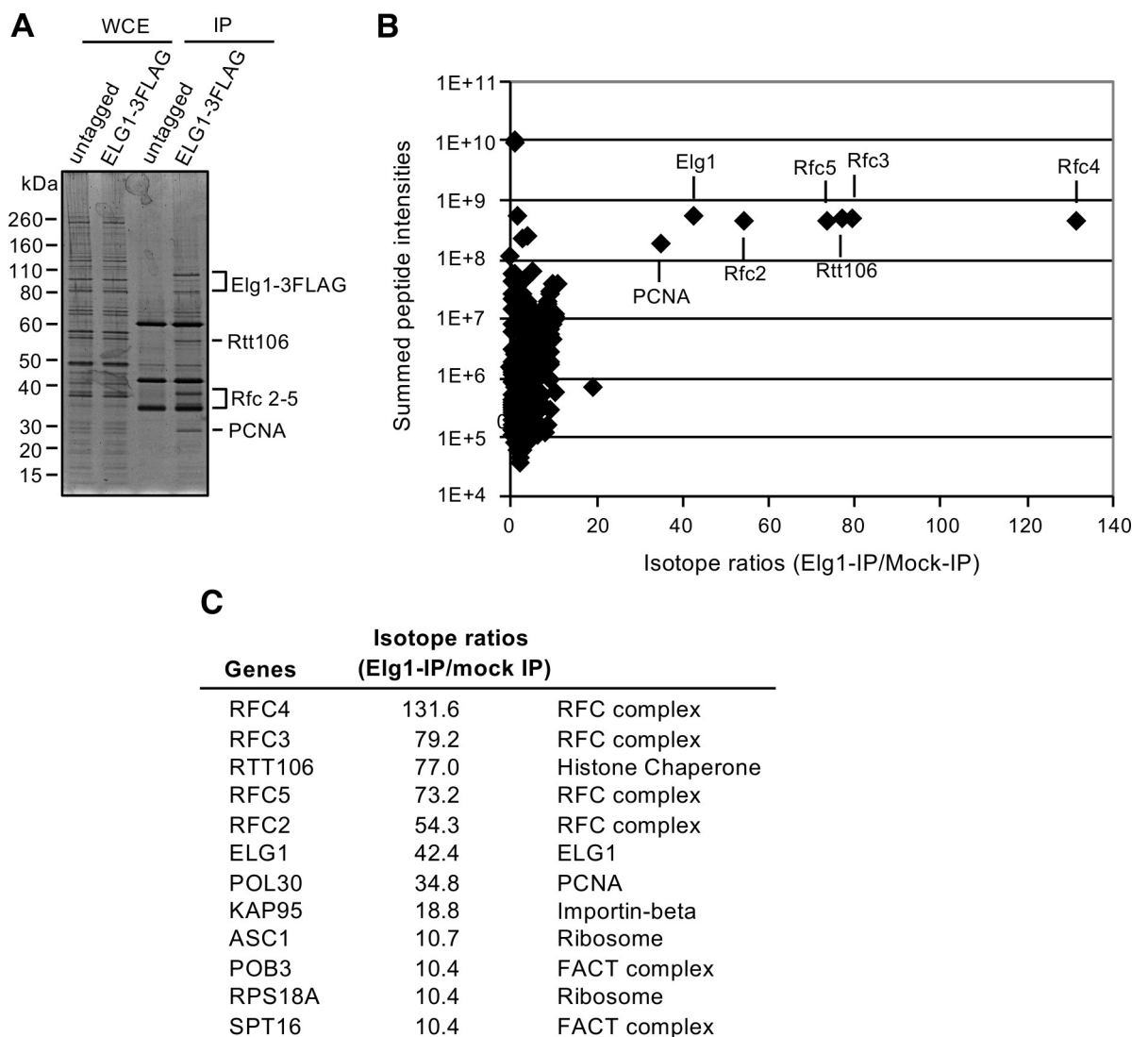


**Fig 4. Rtt106 is identified as Elg1-binding protein by SILAC-IP.** A. Untagged or Elg1-3FLAG tagged strains were differentially labelled with light or heavy lysine and arginine respectively. Following immunoprecipitation with anti-FLAG antibody, IP samples were analysed by SDS-PAGE followed by SYPRO Ruby staining. B & C. Isotope ratios (Elg1-IP/mock IP) and peptide intensities of the proteins identified by SILAC-IP. Rtt106 is enriched at levels similar to those for the RFC2-5 subunits of Elg1 complex.

<https://doi.org/10.1371/journal.pgen.1007783.g004>

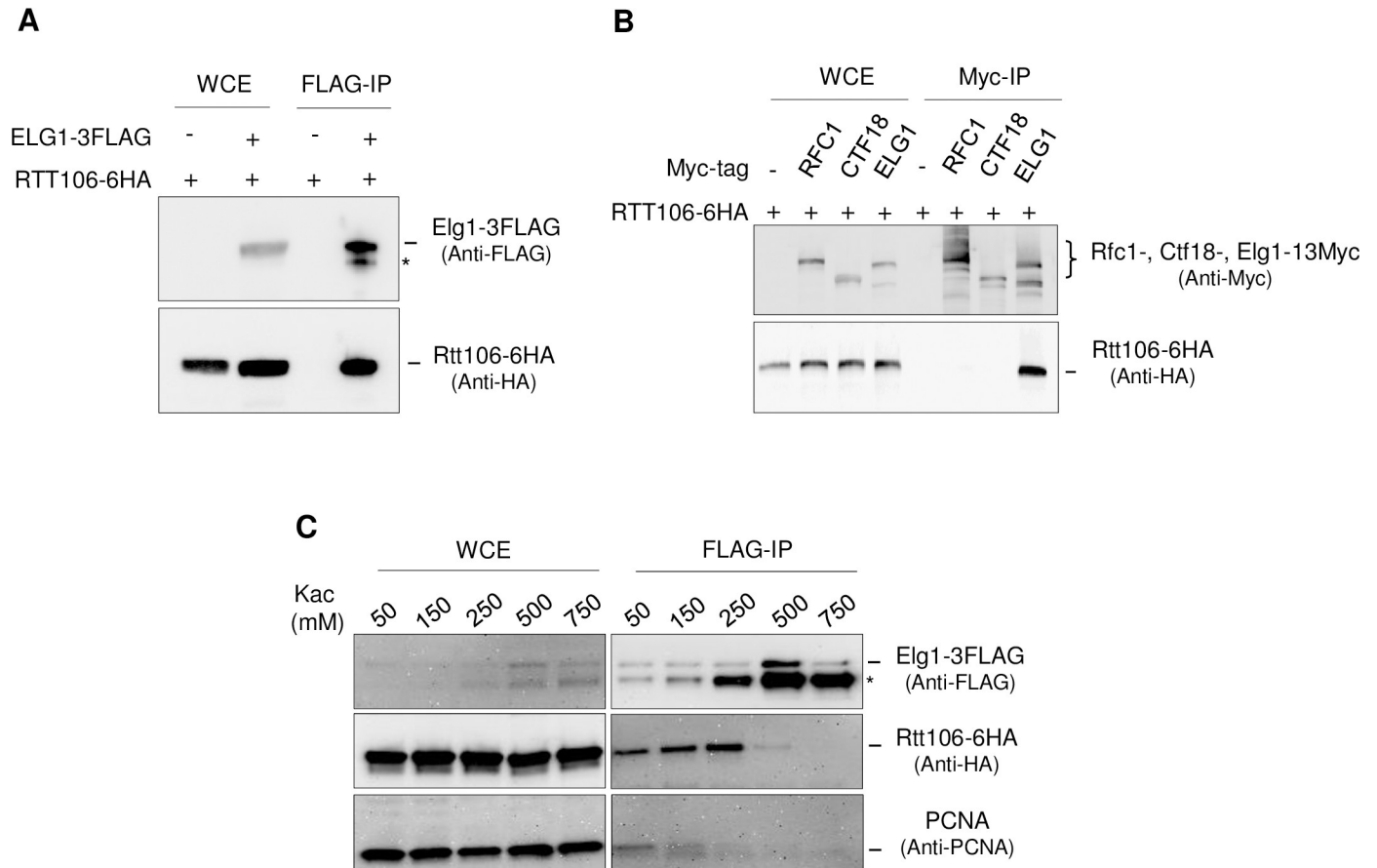


**Fig 5. Rtt106 interacts with Elg1 but not other RFC like complexes.** A. Confirmation of the interaction between Elg1 and Rtt106 by FLAG-IP and Western blot analysis. Asterisk denotes a degradation product. B. Co-immunoprecipitation experiments showing Rtt106 interacts with Elg1 but not the major subunits of other RFC-like complexes, RFC1 and CTF18. C. Co-immunoprecipitation under different salt concentrations (potassium acetate as indicated) shows interaction of Elg1 with Rtt106 is not mediated by PCNA (also, see *S7 Fig*). Asterisk denotes degradation product.

<https://doi.org/10.1371/journal.pgen.1007783.g005>

Immunoprecipitation of Elg1-FLAG pulled down not only Rtt106 but also PCNA, reflecting the function of Elg1-RLC as the major PCNA unloader. Co-immunoprecipitation experiments in the presence of increasing salt concentrations showed that interaction with PCNA was lost at a concentration where Rtt106-Elg1 interaction was retained (*Fig 5C*, 250mM potassium acetate & *S7 Fig*), indicating that the Elg1-Rtt106 interaction is not mediated through PCNA. Note that a band appearing in Western analysis slightly below full-length Elg1 (*Fig 5A*, *5B* & *5C*) appears to represent a degradation product whose appearance is stimulated by increased salt concentration. To summarize, our results indicate that robust interaction occurs between Elg1 and Rtt106, specific to Elg1 amongst the RFC-related complexes.

Since Elg1 is important for nucleosome deposition and interacts with Rtt106, we reasoned that, during DNA replication on the lagging strand, Elg1 might concomitantly recruit Rtt106 as it unloads PCNA, thereby coupling PCNA unloading and chromatin re-assembly. Alternatively, Rtt106 might participate in the PCNA unloading function of Elg1. Examining the accumulation of PCNA on chromatin in the absence of Rtt106 (*S8 Fig*) did not show clear evidence for a role for Rtt106 in PCNA unloading. We therefore followed up the possibility that Elg1 interaction is important to recruit Rtt106 for chromatin re-assembly, by investigating whether recruitment of Rtt106 to replicating regions is dependent on Elg1. We carried out ChIP-seq

analysis of HA-tagged Rtt106 on cells released into hydroxyurea from a G1 arrest. However contrary to our expectation, we did not consistently observe association of Rtt106 with newly replicated regions at early origins (e.g. ARS306, ARS510, ARS310, [S9B Fig](#)). Nor did we observe convincing Rtt106 recruitment to replicating chromatin in a similar experiment carried out under unperturbed conditions (i.e. in WT cells with no HU treatment). Our ChIP experiments did effectively identify Rtt106 binding as we did observe Rtt106 localization at the promoter *HTA1-HTB1* promoter ([S9A Fig](#)), as previously described [37]. Rtt106 recruitment to the *HTA1-HTB1* promoter was not affected in the absence of Elg1 ([S9A Fig](#)). We did notice Rtt106 association with the promoters of some genes encoding putative drug exporters, that in some cases appeared Elg1-dependent. This promoter association does not appear replication-linked, since it was observed at some late-replicating regions that forks will not reach under the HU block conditions of the experiment. The importance of Rtt106 promoter binding will be described elsewhere.

### Defective nucleosome organization in the absence of Elg1 is caused mainly by PCNA retention on DNA

Given the effect of Elg1 on chromatin re-assembly and its interaction with Rtt106, we tested whether the two proteins act in chromatin re-assembly in the same pathway. Specifically, we examined whether the *elg1Δ* and *rtt106Δ* mutations have similar effects on the length of Okazaki fragments. We found that *rtt106Δ* causes only mild lengthening of Okazaki fragments, the degree of lengthening much less than observed for *elg1Δ*. Moreover, the effect of *elg1Δ rtt106Δ* double mutation on Okazaki fragments appeared to be additive rather than epistatic when compared to the single mutations ([Fig 6A](#)). These effects suggest that Elg1 acts in a distinct pathway from Rtt106. Hence, we considered other mechanisms through which *elg1Δ* might affect chromatin re-assembly. The absence of Elg1 results in prolonged accumulation of PCNA on chromatin [11], which could potentially interfere with nucleosome deposition causing defective chromatin re-organization. To investigate this possibility, we made use of trimer instability mutations in PCNA. These mutations cause the PCNA ring to be disassembly-prone, falling off DNA spontaneously even in the absence of Elg1 and thereby suppressing the PCNA accumulation phenotype of the *elg1Δ* mutant [11]. Okazaki fragment length assays were performed in double mutants where *elg1Δ* was combined with two different trimer instability PCNA mutants, *pol30-R14E* (Paul Solomon Devakumar et al. *in revision*) and *pol30-D150E* [11]. We observed that in these double mutants, Okazaki fragments were restored to normal length, when compared to the elongated Okazaki fragments of the *elg1Δ* single mutant ([Fig 6B & S10 Fig](#)). Based on this observation, we propose that when normal PCNA unloading fails due to absence of Elg1, aberrant PCNA accumulation on the newly replicated DNA leads to defective nucleosome deposition.

### Discussion

In this investigation, we show that Elg1 contributes to proper nucleosome assembly across the genome after DNA replication, as evidenced by Okazaki fragment lengthening ([Fig 1](#)) and elevated sensitivity of nascent DNA to micrococcal nuclease digestion ([Figs 2 & 3](#)) in an *elg1Δ* mutant. Okazaki fragment length has previously been examined in several studies as a proxy for nucleosome deposition [32]. This assay could raise the concern that the DNA ligase-deficient background required to visualize Okazaki fragments might itself impact on fragment length or nucleosome re-assembly, but a different study [38] obtained consistent results, also finding that nucleosome position determines *S. cerevisiae* Okazaki fragment positioning, using a completely different approach that analyzed mutations inserted by an error-prone polymerase  $\alpha$  prone to

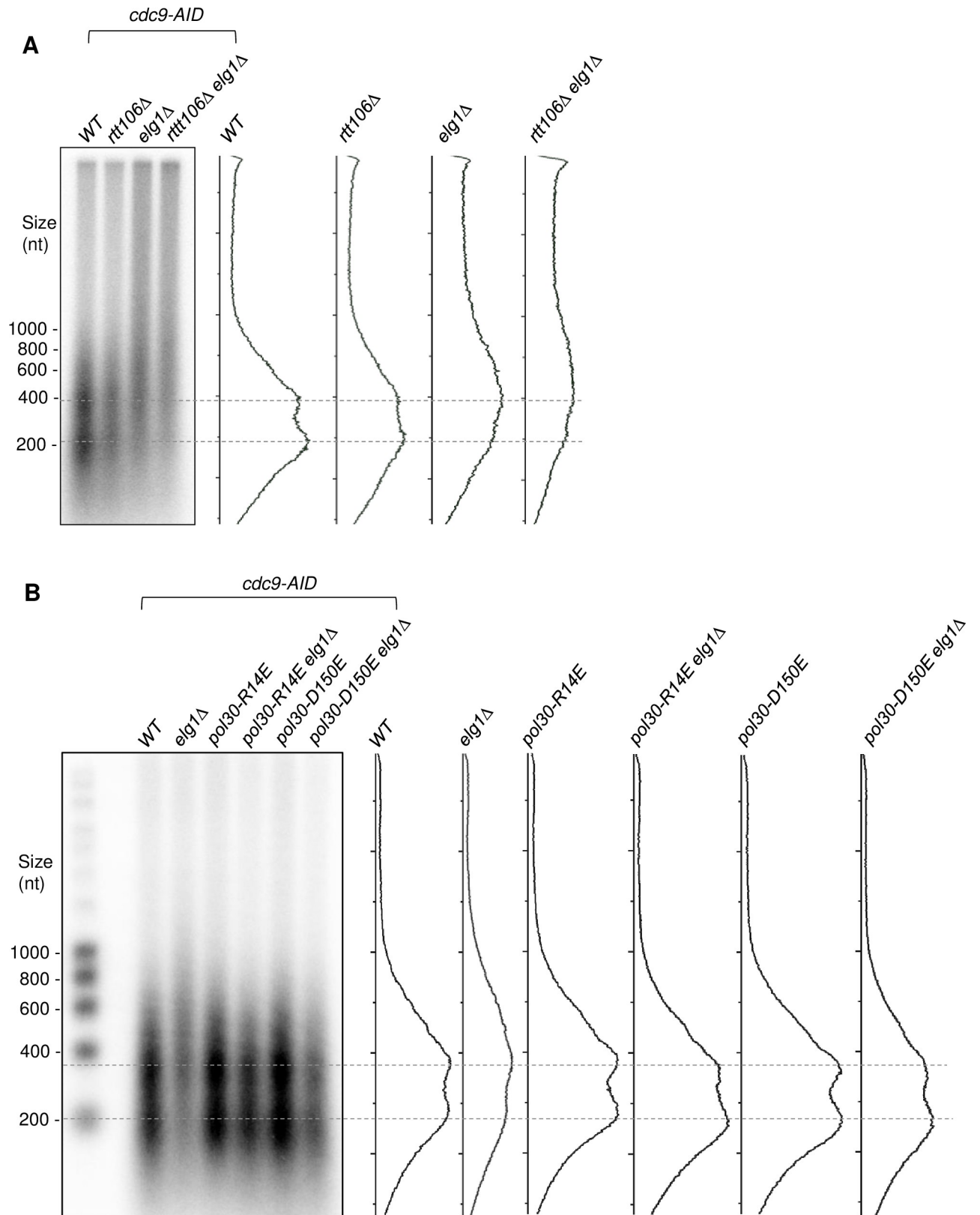


**Fig 6. Extended Okazaki fragments in the *elg1Δ* mutant are rescued by disassembly-prone mutants of PCNA.** A. Okazaki fragments are extended less in *rtt106Δ* mutant than in *elg1Δ*, suggesting that Elg1 affects Okazaki fragment length independent of Rtt106. B. Disassembly-prone mutant of

PCNA (*pol30-R14E* or *pol30-D150E*) rescue the Okazaki fragment length extension observed in *elg1Δ*. Dotted lines show Okazaki fragments corresponding to mono- and di-nucleosome sizes. Trace of signal intensity for each lane is shown.

<https://doi.org/10.1371/journal.pgen.1007783.g006>

ribonucleotide insertion. Moreover, in assays that measure the micrococcal nuclease sensitivity of nascent DNA (in cells where DNA ligase activity is intact) we confirmed that nucleosome deposition is affected by the *elg1Δ* mutation. Therefore, the Okazaki fragment lengthening phenotype indeed reflects a nascent strand chromatin re-assembly defect.

To understand interactions that may contribute to the chromatin re-assembly effect of Elg1, we examined the proteins that co-precipitate with Elg1 in pull-down experiments, and identified novel interactions of Elg1 with histone chaperones, in particular Rtt106 and the FACT complex. Interestingly, Rtt106 appears to bind the Elg1-RLC in almost stoichiometric amounts, in an interaction that does not depend on PCNA. Rtt106 does not interact with either Rfc1 or Ctf18. Consistently, we found that both the N-terminal and C-terminal regions that are unique to Elg1 are needed for Rtt106 interaction (S6 Fig).

To examine the extent to which Rtt106-Elg1 interaction versus the Elg1 PCNA unloading function are important for chromatin re-assembly, we made use of disassembly-prone mutants of PCNA which do not accumulate on chromatin even in the absence of Elg1. Using these mutations to relieve PCNA accumulation on chromatin in an *elg1Δ* background restored Okazaki fragments to normal length, indicating that prompt and effective PCNA unloading is absolutely essential for normal nucleosome deposition in the wake of replication forks.

How might PCNA accumulation result in defective nucleosome assembly and associated Okazaki fragment lengthening? Okazaki fragment length is proposed to be regulated by nucleosome deposition on the previously synthesized section of DNA [13,38] as illustrated in Fig 7. The newly deposited nucleosome on the last piece of DNA synthesized is believed to form an obstacle to progression of polymerase  $\delta$  as it carries out strand displacement synthesis, prior to completing synthesis of each Okazaki fragment. Encounter of pol  $\delta$  with the nucleosome is suggested to favour pol  $\delta$  disengagement and dissociation, allowing PCNA to recruit DNA ligase [39] with ligation of the completed Okazaki fragment to the nascent lagging strand determining the final Okazaki fragment length (Fig 7, Model i). We propose that in the absence of Elg1, accumulated PCNA in the wake of the replisome obstructs normal placement and spacing of nucleosome deposition, so that the nucleosomal barrier to pol  $\delta$  synthesis is not present, resulting in longer Okazaki fragments being synthesized prior to their eventual completion and ligation (Fig 7, Model ii). Combining the *elg1Δ* mutation with a PCNA trimer-unstable mutant prevents the accumulation of PCNA, relieving the block to nucleosome deposition and restoring the normal mechanism of Okazaki fragment length determination (Fig 7, Model iii).

Our findings support the suggestion that nucleosome deposition is a very early event that precedes and stimulates pol  $\delta$  dissociation, the polymerase in turn allowing DNA ligase recruitment by PCNA [39] and subsequent Okazaki fragment ligation, which is necessary for PCNA unloading by the Elg1-RLC. Our results are therefore consistent with the previously identified dependence of PCNA unloading on Okazaki fragment ligation [6].

A very recent study by [40] provides an interesting illustration of the consequences of disrupting PCNA removal by Elg1-RLC and nucleosome deposition. Janke et al used an assay that measures heterochromatin disruption, by testing for failure to silence expression of a Cre recombinase gene. Their finding that silencing is disrupted by an *elg1Δ* mutation (or by histone chaperone mutations) implies that normal replication-coupled chromatin assembly is needed to preserve silencing at a specific heterochromatic locus. Our study generalizes the conclusion that Elg1 activity is needed for normal chromatin inheritance, with the

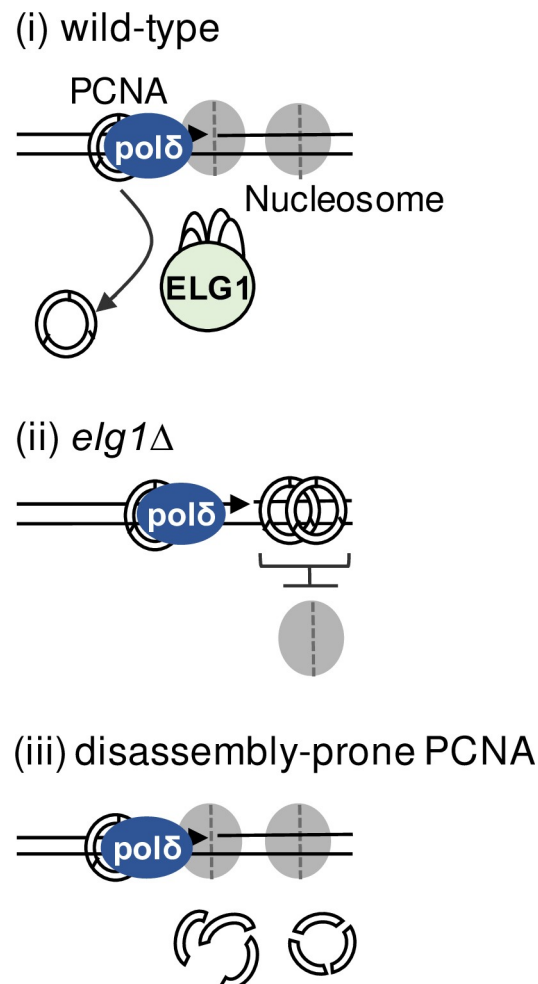


**Fig 7. Model for the role of Elg1 in chromatin re-organization in lagging strand replication.**

<https://doi.org/10.1371/journal.pgen.1007783.g007>

discovery that nucleosome deposition problems caused by failure to unload PCNA extend genome-wide.

Since delayed PCNA removal appears to be the main cause of the chromatin re-assembly defect observed in *elg1 $\Delta$ , what is the significance of Elg1 interaction with histone chaperones, in particular Rtt106 and FACT complex? Identification of these interactions raises the suggestion that Elg1 might recruit histone chaperones to assist in chromatin re-assembly, with Elg1 thereby contributing to chromatin re-configuration or maturation. However, our ChIP analysis failed to identify a clear role for Elg1 in localizing Rtt106 to newly synthesized DNA. We did find that Elg1 has effects on Rtt106 chromatin association at the promoters of a number of genes, particularly genes involved in cellular transport and drug resistance. However, this effect is unlikely to be coupled to DNA replication since we observed Rtt106 association with several such sites in G1 phase samples. Slight sensitivity of an *elg1 $\Delta$  mutant to HU [8] would be consistent with a need for Elg1 in controlling the expression of genes required for drug response and export. The possibility of a non-replication-associated role for Elg1 in regulating gene expression through histone chaperone recruitment is the subject of ongoing study.**

While PCNA accumulation appears to be the immediate cause of delayed nucleosome deposition in the *elg1 $\Delta$  mutant (Fig 7), our results do not exclude the possibility of a role for*

Rtt106-Elg1 in replication-coupled chromatin re-establishment, especially since presence of multiple, redundant histone chaperones activities in yeast complicates analysis of chromatin re-assembly. However, we could not obtain unambiguous, reproducible evidence of a role for Elg1-Rtt106 interaction following replication. One possibility is that Elg1 does contribute to coordination of chromatin re-assembly, operating through Rtt106 and/or other histone chaperones, in a pathway acting at a later stage of chromatin maturation operating after histone deposition and Okazaki fragment ligation.

The role of Elg1 appears to be conserved, since its mammalian homolog, called ATAD5, also appears to mediate PCNA unloading [41]. Mammalian cells lacking ATAD5 show PCNA accumulation on chromatin similar to that observed in yeast, and it seems likely that such PCNA retention may impact chromatin re-assembly. The major phenotype of mice lacking ATAD5 is cancer predisposition, and indeed ATAD5 mutations are also proposed to contribute to human ovarian cancers [42,43]. Defects in genomic function caused by derailed chromatin re-assembly following replication might therefore contribute significantly to human cancer development or progression.

## Materials and methods

### Yeast strains

All yeast strains used in this study are listed in [S1 Table](#). Gene disruptions and epitope tags were introduced by standard PCR based methods [44,45].

### Detection of Okazaki fragments

Okazaki fragment purification and detection was performed as described previously in [13].

### Analysis of nascent chromatin structure by micrococcal nuclease digestion

Yeast cells were grown to  $OD_{600}$  of 0.2 at 30°C in 60ml YPD media and then alpha factor was added to arrest cells in G1 phase. 400µg/ml BrdU was added to the culture and incubated for 30 minutes for cells to take up BrdU. Cells were then released into S phase by resuspending in fresh YPD containing 400µg/ml BrdU. Then 20 ml samples were collected at desired time points into formaldehyde (1% final concentration) and incubated with rotation for 15 minutes at room temperature. 125mM glycine was then added to neutralise formaldehyde. Cells were washed twice in 10 ml of ice cold 1X PBS, then with 2 ml of spheroplasting buffer (1M sorbitol, 1mM beta-mercaptoethanol) before resuspending in 1ml of spheroplasting buffer with 300µg/ml 100-T Zymolase then incubated at 30°C for 20 minutes. Spheroplasts were washed in 1ml of spheroplasting buffer and resuspended in 600µl of Digestion buffer (1M sorbitol, 50mM NaCl, 10mM Tris-HCl pH7.4, 5mM MgCl<sub>2</sub>, 5mM CaCl<sub>2</sub>, 0.075% Nonidet P-40, 1mM beta-mercaptoethanol, 0.5mM spermidine). 200µl aliquots were subjected to micrococcal nuclease (NEB, M0247S) digestion (200 or 600 gel units) for 5 minutes at 37°C. Digestions were stopped by adding 1/10 volume of stop solution (250mM EDTA, 5% SDS). 5µl of 20 mg/ml Proteinase K was added and incubated overnight at 55°C. Following phenol-chloroform extraction, DNA was precipitated using 1/10 volume of 3M sodium acetate and 2 volumes of 100% ethanol. The air-dried DNA pellet was resuspended in 20µl of TE buffer with RNase A (1mg/ml) and incubated for 2 hours at 37°C. DNA samples were electrophoresed on a 1.4% agarose gel, which was incubated in denaturing buffer (0.5M NaOH, 1M NaCl) twice for 15 minutes followed by incubation in neutralization buffer (0.5M Tris-HCl, 3M NaCl) for 30 minutes. The DNA was then transferred to Amersham Hybond N<sup>+</sup> membrane by Southern blotting. DNA was cross-

linked to the membrane with UV light (1200J). The membrane was then incubated in 5% milk in TBS-tween for 60 minutes and probed with anti-BrdU antibody (ab12219, abcam).

### Protein affinity techniques

Whole cell extract preparation, western blotting and co-immunoprecipitation experiments were performed as described previously [5,6]. Antibodies used were: anti-BrdU (ab12219, abcam), anti-FLAG (F1804, Sigma), anti-HA (HA.11 clone 16B12, Covance), anti-PCNA (ab70472, abcam).

### SILAC-mass spectrometry

SILAC Quantitative proteomic analysis was performed as described previously [46].

### ChIP-seq analysis

Yeast strains were grown to an OD<sub>600</sub> of 0.25 in YPD. Alpha factor was added to arrest cells in G1 and released into YPD containing 0.2M hydroxyurea at 23°C for 60 minutes. Formaldehyde (1% final concentration) was added and incubated with rotation first at room temperature for 20 minutes and then at 4°C overnight. Cells were washed 3 times with ice-cold 1X Phosphate buffered saline. Cells were pelleted and frozen at -80°C. Rtt106 ChIP using anti-HA (HA.11 clone 16B12, Covance) and data analysis were performed as described previously [6].

ChIP-Seq data are uploaded to Array Express under accession number: E-MTAB-6985

### MNase-seq analysis

**Chromatin digestion and EdU pulldown.** Yeast cells were grown to an OD<sub>600</sub> of 0.66 at 30°C, then incubated with alpha factor for 2.5 hours at 30°C. Cells were then released into YPD containing 50μM EdU at room temperature. Samples were collected at indicated time points into formaldehyde (1% final concentration) and incubated for 10 minutes, followed by quenching with 125 mM glycine for 5 minutes. Cells were chilled on ice, washed 3X with cold Tris-buffered saline (20mM Tris pH 7.5, 120 mM NaCl), pelleted and frozen at -80°C. Frozen cell pellets were resuspended in ice cold Spheroplast Digestion Buffer (1M Sorbitol, 50mM NaCl, 10mM Tris-HCl pH 7.5, 5mM MgCl<sub>2</sub>, 1mM CaCl<sub>2</sub>, and 0.075% v/v Nonidet P-40 Substitute supplemented with 1mM 2-mercaptoethanol, and 0.5mM of each of the following: Spermidine, Pepstatin, Aprotinin, benzamidine, E64, and ABSF) then lysed in a Mini-Bead Beater 8 at 4°C. MNase was titrated to give 80% mononucleosomal DNA bands, typically 30 units for 15 minutes at 37°C. Samples were incubated overnight at 65°C with proteinase K and the supernatant was treated with RNase A for 1h at 37°C, followed by phenol-chloroform extraction and isopropanol precipitation. Excised mononucleosome bands from an agarose size-selection gel were purified using Freeze-n-Squeeze columns followed by phenol-chloroform extraction and cold ethanol precipitation.

A Click-iT NascentRNACapture Kit (Invitrogen, C10365) was used to biotinylate EdU-labelled nascent DNA, which was pulled down with Streptavidin MyOne Dynabeads (Invitrogen, 65601) according to Invitrogen protocols.

**High throughput sequencing library construction & Data analysis.** DNA was blunt-ended, an A-overhang was added, and Illumina adapters were ligated on, with Agencourt Ampure XP bead washes after each step. PCR amplification was performed with 18 or fewer cycles using Illumina barcoded primers and primer PE 1.0, followed by a final Ampure bead purification. Adapter Sequences used: Top PE Adapter (ACACTCTTTCCCTACACGACGCTCTTCCGATC\*T) Bottom PE Adapter (P-GATCGGAAGAGCGGTTCAGCAGGAATG

CCGAG) PE 1.0 (AATGATACGGCGACCACCGAGATCTACACTCTTTCCCTACACGACGCTCTTCCGATCT).

Reads were mapped to the *S. cerevisiae* genome using Bowtie2. Replication origin [47] and TSS data was generated and graphed using custom Python scripts, with strand orientation accounted for in the analysis. Data were normalized by dividing by mean read depth per base pair and plots were smoothed with a 50bp sliding window.

MNase-Seq data are uploaded to Array Express under accession number: E-MTAB-6985

## Supporting information

**S1 Fig. Biological repeat of Fig 1C.** Okazaki Fragment length assay showing Okazaki fragments are extended in *elg1Δ*, similar to *cac2Δ* and unlike *ctf18Δ*. Dotted lines show Okazaki fragments corresponding to mono- and di-nucleosome sizes. Trace of signal intensity for each lane is shown.

(TIF)

**S2 Fig.** Micrococcal nuclease digestion of nascent chromatin reveals defective nucleosome assembly in *elg1Δ* (A) & (B) and *cac1Δ* (C) compared to WT. Signal traces represent 45 min nascent DNA sample lanes (highest concentration of MNase lane) revealing increased mono-nucleosomal DNA in the mutants when compared to WT. MNase digestion experiments were performed as described in Fig 2. Panel A & B shows biological repeats of Fig 2C.

(TIF)

**S3 Fig. Flow cytometry profiles show no difference in S phase progression in WT and *elg1Δ*.** Cells were arrested in G1 using alpha factor and released into S phase at 30°C and samples were collected at indicated time-points for flow-cytometry analysis.

(TIF)

**S4 Fig.** Genome-wide MNase-seq analysis shows defective nucleosome organization in *elg1Δ* (A) and *cac1Δ* (B). Nascent DNA nucleosomal reads (as in Fig 3) aligned to Transcription Start Sites (TSS). G1 samples show total DNA, and 27.5–60 min samples nascent DNA recovered by EdU pulldown. Plots in panel A show the mean of two biological repeats, whereas plots in panel B are from one experiment.

(TIF)

**S5 Fig.** Biological replicates (A & B) showing genome-wide MNase-seq analysis, revealing defective nucleosome organization in *elg1Δ*. Nucleosomal reads on nascent DNA aligned to replication origins (ARS). G1 samples show total DNA, whereas 27.5–60 min samples show nascent DNA recovered by EdU pulldown. Fig 3B shows the mean of these two biological repeats.

(TIF)

**S6 Fig. Both N-terminal and C-terminal domains of Elg1 are important for interaction with Rtt106.** A. Immunoprecipitation experiment to map domains of Elg1 interacting with Rtt106. WT Elg1 and Elg1 fragments were expressed from the endogenous locus and promoter. Elg1-3FLAG immunoprecipitation was performed as described previously [11]. PCNA interaction data as shown in [11]. B. Schematic structure of Elg1 and truncation mutants, with strength of Rtt106 interaction indicated.

(TIF)

**S7 Fig. Co-immunoprecipitation under different salt concentrations (potassium acetate as indicated) shows interaction of Elg1 with Rtt106 is not mediated by PCNA.** Asterisk

denotes degradation product.  
(TIF)

**S8 Fig. PCNA on chromatin is slightly increased in *rtt106Δ* compared to WT, but not to the extent of *elg1Δ*.** (A). Whole cell extract and chromatin fractions from indicated strains were prepared and analysed by western blotting. Plots showing quantification of the relative amounts of unmodified PCNA in Whole Cell Extract (WCE) and Chromatin (Ch) (B) and K164-SUMO PCNA (C) in the mutant strains compared to WT. K164-SUMO PCNA is a marker of chromatin association. Whole cell extract and chromatin-enriched fraction prepared as described previously [6].

(TIF)

**S9 Fig.** ChIP-Seq experiment showing Rtt106-6HA recruitment at promoter region of *HTA1-HTB1* (A) and origins of replication (B).

(TIF)

**S10 Fig. Biological replicate of the experiment shown in Fig 6.** Disassembly-prone mutant of PCNA (*pol30-R14E* or *pol30-D150E*) rescue the Okazaki fragment length extension observed in *elg1Δ*. Dotted lines show Okazaki fragments corresponding to mono- and di-nucleosome sizes. Trace of signal intensity for each lane is shown.

(TIF)

**S1 Table. Yeast strains used in this study.**

(XLSX)

**S1 Dataset. SILAC-based quantitative mass spectrometry analysis for identification of Elg1 interaction partners.**

(XLSX)

## Acknowledgments

We thank members of the Donaldson, Kubota, and Lorenz labs for helpful discussion, Sophie Shaw at the University of Aberdeen for data upload to Array Express and Shin-ichiro Hiraga for help with Bioinformatic analysis.

## Author Contributions

**Conceptualization:** Vamsi K. Gali, Takashi Kubota, Anne D. Donaldson.

**Formal analysis:** Vamsi K. Gali, David Dickerson, Yuki Katou, Katsunori Fujiki, Katsuhiko Shirahige, Tom Owen-Hughes, Takashi Kubota, Anne D. Donaldson.

**Funding acquisition:** Katsuhiko Shirahige, Tom Owen-Hughes, Anne D. Donaldson.

**Investigation:** Vamsi K. Gali, David Dickerson, Yuki Katou, Katsunori Fujiki, Takashi Kubota, Anne D. Donaldson.

**Methodology:** Vamsi K. Gali, David Dickerson, Yuki Katou, Takashi Kubota, Anne D. Donaldson.

**Project administration:** Anne D. Donaldson.

**Resources:** Katsuhiko Shirahige, Tom Owen-Hughes, Anne D. Donaldson.

**Supervision:** Katsuhiko Shirahige, Tom Owen-Hughes, Takashi Kubota, Anne D. Donaldson.

**Validation:** Vamsi K. Gali, David Dickerson, Yuki Katou.

**Visualization:** Vamsi K. Gali, David Dickerson, Yuki Katou.

**Writing – original draft:** Vamsi K. Gali.

**Writing – review & editing:** Anne D. Donaldson.

## References

1. Groth A, Rocha W, Verreault A, Almouzni G. Chromatin Challenges during DNA Replication and Repair. *Cell*. 2007; pp. 721–733. <https://doi.org/10.1016/j.cell.2007.01.030> PMID: 17320509
2. Mailand N, Gibbs-Seymour I, Bekker-Jensen S. Regulation of PCNA–protein interactions for genome stability. *Nat Rev Mol Cell Biol*. 2013; 14: 269–282. <https://doi.org/10.1038/nrm3562> PMID: 23594953
3. Bowman GD, O'Donnell M, Kuriyan J. Structural analysis of a eukaryotic sliding DNA clamp–clamp loader complex. *Nature*. 2004; 429: 724–730. <https://doi.org/10.1038/nature02585> PMID: 15201901
4. Gomes X V., Burgers PMJ. ATP utilization by yeast replication factor C: I. ATP-mediated interaction with DNA and with proliferating cell nuclear antigen. *J Biol Chem*. 2001; 276: 34768–34775. <https://doi.org/10.1074/jbc.M011631200> PMID: 11432853
5. Kubota T, Nishimura K, Kanemaki MT, Donaldson AD. The Elg1 Replication Factor C-like Complex Functions in PCNA Unloading during DNA Replication. *Mol Cell*. 2013; 50: 273–280. <https://doi.org/10.1016/j.molcel.2013.02.012> PMID: 23499004
6. Kubota T, Katou Y, Nakato R, Shirahige K, Donaldson AD. Replication-Coupled PCNA Unloading by the Elg1 Complex Occurs Genome-wide and Requires Okazaki Fragment Ligation. *Cell Rep*. 2015; 12: 774–787. <https://doi.org/10.1016/j.celrep.2015.06.066> PMID: 26212319
7. Bellaoui M, Chang M, Ou J, Xu H, Boone C, Brown GW. Elg1 forms an alternative RFC complex important for DNA replication and genome integrity. *EMBO J*. 2003; 22: 4304–4313. <https://doi.org/10.1093/emboj/cdg406> PMID: 12912927
8. Ben-Aroya S, Koren A, Liefshitz B, Steinlauf R, Kupiec M. ELG1, a yeast gene required for genome stability, forms a complex related to replication factor C. *Proc Natl Acad Sci U S A*. 2003; 100: 9906–9911. <https://doi.org/10.1073/pnas.1633757100> PMID: 12909721
9. Smolnikov S, Mazor Y, Krauskopf A. ELG1, a regulator of genome stability, has a role in telomere length regulation and in silencing. *Proc Natl Acad Sci*. 2004; 101: 1656–1661. <https://doi.org/10.1073/pnas.0307796100> PMID: 14745004
10. Parnas O, Zipin-Roitman A, Mazor Y, Liefshitz B, Ben-Aroya S, Kupiec M. The Elg1 clamp loader plays a role in sister chromatid cohesion. *PLoS One*. 2009; 4. <https://doi.org/10.1371/journal.pone.0005497> PMID: 19430531
11. Johnson C, Gali VK, Takahashi TS, Kubota T. PCNA Retention on DNA into G2/M Phase Causes Genome Instability in Cells Lacking Elg1. *Cell Rep*. 2016; 16: 684–695. <https://doi.org/10.1016/j.celrep.2016.06.030> PMID: 27373149
12. Stillman B. Chromatin assembly during SV40 DNA replication in vitro. *Cell*. 1986; 45: 555–565. doi:0092-8674(86)90287-4 [pii] PMID: 3011272
13. Smith DJ, Whitehouse I. Intrinsic coupling of lagging-strand synthesis to chromatin assembly. *Nature*. 2012; 483: 434–438. <https://doi.org/10.1038/nature10895> PMID: 22419157
14. Hammond CM, Strømme CB, Huang H, Patel DJ, Groth A. Histone chaperone networks shaping chromatin function. *Nature Reviews Molecular Cell Biology*. 2017. <https://doi.org/10.1038/nrm.2016.159> PMID: 28053344
15. Wittmeyer J, Joss L, Formosa T. Spt16 and Pob3 of *Saccharomyces cerevisiae* form an essential, abundant heterodimer that is nuclear, chromatin-associated, and copurifies with DNA polymerase alpha. *Biochemistry*. 1999; 38: 8961–8971. <https://doi.org/10.1021/bi982851d> PMID: 10413469
16. Tan BC-M, Chien C-T, Hirose S, Lee S-C. Functional cooperation between FACT and MCM helicase facilitates initiation of chromatin DNA replication. *EMBO J*. 2006; 25: 3975–3985. <https://doi.org/10.1038/sj.emboj.7601271> PMID: 16902406
17. Foltman M, Evrin C, De Piccoli G, Jones RC, Edmondson RD, Katou Y, et al. Eukaryotic replisome components cooperate to process histones during chromosome replication. *Cell Rep*. 2013; 3: 892–904. <https://doi.org/10.1016/j.celrep.2013.02.028> PMID: 23499444
18. Yang J, Zhang X, Feng J, Leng H, Li S, Xiao J, et al. The Histone Chaperone FACT Contributes to DNA Replication-Coupled Nucleosome Assembly. *Cell Rep*. 2016; 14: 1128–1141. <https://doi.org/10.1016/j.celrep.2015.12.096> PMID: 26804921

19. Li Q, Zhou H, Wurtele H, Davies B, Horazdovsky B, Verreault A, et al. Acetylation of Histone H3 Lysine 56 Regulates Replication-Coupled Nucleosome Assembly. *Cell*. 2008; 134: 244–255. <https://doi.org/10.1016/j.cell.2008.06.018> PMID: 18662540
20. Franco AA, Lam WM, Burgers PM, Kaufman PD. Histone deposition protein Asf1 maintains DNA replisome integrity and interacts with replication factor C. *Genes Dev*. 2005; 19: 1365–1375. <https://doi.org/10.1101/gad.1305005> PMID: 15901673
21. Sauer P V, Gu Y, Liu WH, Mattioli F, Panne D, Luger K, et al. Mechanistic insights into histone deposition and nucleosome assembly by the chromatin assembly factor-1. *Nucleic Acids Res*. Oxford University Press; 2018; 1–11. <https://doi.org/10.1093/nar/gkx1156> PMID: 29177436
22. Shibahara K, Stillman B. Replication-dependent marking of DNA by PCNA facilitates CAF-1-coupled inheritance of chromatin. *Cell*. 1999; 96: 575–585. [https://doi.org/10.1016/S0092-8674\(00\)80661-3](https://doi.org/10.1016/S0092-8674(00)80661-3) PMID: 10052459
23. Moggs JG, Grandi P, Quivy JP, Jónsson ZO, Hübscher U, Becker PB, et al. A CAF-1-PCNA-mediated chromatin assembly pathway triggered by sensing DNA damage. *Mol Cell Biol*. 2000; 20: 1206–18. <https://doi.org/10.1128/MCB.20.4.1206-1218.2000> PMID: 10648606
24. Zhang K, Gao Y, Li J, Burgess R, Han J, Liang H, et al. A DNA binding winged helix domain in CAF-1 functions with PCNA to stabilize CAF-1 at replication forks. *Nucleic Acids Res*. 2016; 44: 5083–5094. <https://doi.org/10.1093/nar/gkw106> PMID: 26908650
25. Su D, Hu Q, Li Q, Thompson JR, Cui G, Fazly A, et al. Structural basis for recognition of H3K56-acetylated histone H3-H4 by the chaperone Rtt106. *Nature*. 2012; <https://doi.org/10.1038/nature10861> PMID: 22307274
26. Fazly A, Li Q, Hu Q, Mer G, Horazdovsky B, Zhang Z. Histone chaperone Rtt106 promotes nucleosome formation using (H3-H4)<sub>2</sub>tetramers. *J Biol Chem*. 2012; <https://doi.org/10.1074/jbc.M112.347450> PMID: 22337870
27. Zunder RM, Antczak AJ, Berger JM, Rine J. Two surfaces on the histone chaperone Rtt106 mediate histone binding, replication, and silencing. *Proc Natl Acad Sci*. 2012; 109: E144–E153. <https://doi.org/10.1073/pnas.1119095109> PMID: 22198837
28. Huang S, Zhou H, Katzmann D, Hochstrasser M, Atanasova E, Zhang Z. Rtt106p is a histone chaperone involved in heterochromatin-mediated silencing. *Proc Natl Acad Sci*. 2005; 102: 13410–13415. <https://doi.org/10.1073/pnas.0506176102> PMID: 16157874
29. Imbeault D, Gamar L, Rufiange A, Paquet E, Nourani A. The Rtt106 histone chaperone is functionally linked to transcription elongation and is involved in the regulation of spurious transcription from cryptic promoters in yeast. *J Biol Chem*. 2008; 283: 27350–27354. <https://doi.org/10.1074/jbc.C800147200> PMID: 18708354
30. Fillingham J, Kainth P, Lambert JP, van Bakel H, Tsui K, Peña-Castillo L, et al. Two-Color Cell Array Screen Reveals Interdependent Roles for Histone Chaperones and a Chromatin Boundary Regulator in Histone Gene Repression. *Mol Cell*. 2009; 35: 340–351. <https://doi.org/10.1016/j.molcel.2009.06.023> PMID: 19683497
31. Ferreira ME, Flaherty K, Prochasson P. The *Saccharomyces cerevisiae* histone chaperone Rtt106 mediates the cell cycle recruitment of SWI/SNF and RSC to the HIR-dependent histone genes. *PLoS One*. 2011; 6. <https://doi.org/10.1371/journal.pone.0021113> PMID: 21698254
32. Yadav T, Whitehouse I. Replication-Coupled Nucleosome Assembly and Positioning by ATP-Dependent Chromatin-Remodeling Enzymes. *Cell Rep*. 2016; 15: 715–723. <https://doi.org/10.1016/j.celrep.2016.03.059> PMID: 27149855
33. Hanna JS, Kroll ES, Lundblad V, Spencer FA. *Saccharomyces cerevisiae* CTF18 and CTF4 are required for sister chromatid cohesion. *Mol Cell Biol*. 2001; 21: 3144–58. <https://doi.org/10.1128/MCB.21.9.3144-3158.2001> PMID: 11287619
34. Mayer ML, Gygi SP, Aebersold R, Hieter P. Identification of RFC(Ctf18p, Ctf8p, Dcc1p): An alternative RFC complex required for sister chromatid cohesion in *S. cerevisiae*. *Mol Cell*. 2001; 7: 959–970. [https://doi.org/10.1016/S1097-2765\(01\)00254-4](https://doi.org/10.1016/S1097-2765(01)00254-4) PMID: 11389843
35. Fennessy RT, Owen-Hughes T. Establishment of a promoter-based chromatin architecture on recently replicated DNA can accommodate variable inter-nucleosome spacing. *Nucleic Acids Res*. 2016; 44: 7189–7203. <https://doi.org/10.1093/nar/gkw331> PMID: 27106059
36. Burgess RJ, Zhang Z. Histone chaperones in nucleosome assembly and human disease. *Nat Struct Mol Biol*. 2014; 20: 14–22. <https://doi.org/10.1038/nsmb.2461.Histone>
37. Zunder RM, Rine J. Direct Interplay among Histones, Histone Chaperones, and a Chromatin Boundary Protein in the Control of Histone Gene Expression. *Mol Cell Biol*. 2012; 32: 4337–4349. <https://doi.org/10.1128/MCB.00871-12> PMID: 22907759

38. Reijns MAM, Kemp H, Ding J, De Procé SM, Jackson AP, Taylor MS. Lagging-strand replication shapes the mutational landscape of the genome. *Nature*. 2015; 518: 502–506. <https://doi.org/10.1038/nature14183> PMID: 25624100
39. Vijayakumar S, Chapados BR, Schmidt KH, Kolodner RD, Tainer JA, Tomkinson AE. The C-terminal domain of yeast PCNA is required for physical and functional interactions with Cdc9 DNA ligase. *Nucleic Acids Res*. 2007; 35: 1624–1637. <https://doi.org/10.1093/nar/gkm006> PMID: 17308348
40. Janke R, King GA, Kupiec M, Rine J. Pivotal roles of PCNA loading and unloading in heterochromatin function. *Proc Natl Acad Sci*. 2018; 201721573. <https://doi.org/10.1073/pnas.1721573115> PMID: 29440488
41. Lee KY, Fu H, Aladjem MI, Myung K. ATAD5 regulates the lifespan of DNA replication factories by modulating PCNA level on the chromatin. *J Cell Biol*. 2013; 200: 31–44. <https://doi.org/10.1083/jcb.201206084> PMID: 23277426
42. Maleva Kostovska I, Wang J, Bogdanova N, Schürmann P, Bhuju S, Geffers R, et al. Rare ATAD5 missense variants in breast and ovarian cancer patients. *Cancer Lett*. 2016; 376: 173–177. <https://doi.org/10.1016/j.canlet.2016.03.048> PMID: 27045477
43. Bell DW, Sikdar N, Lee KY, Price JC, Chatterjee R, Park HD, et al. Predisposition to cancer caused by genetic and functional defects of mammalian atad5. *PLoS Genet*. 2011; 7. <https://doi.org/10.1371/journal.pgen.1002245> PMID: 21901109
44. Berben G, Dumont J, Gilliquet V, Bolle P-A, Hilger F. The YDp plasmids: A uniform set of vectors bearing versatile gene disruption cassettes for *Saccharomyces cerevisiae*. *Yeast*. 1991; 7: 475–477. <https://doi.org/10.1002/yea.320070506> PMID: 1897313
45. Longtine MS, McKenzie A, Demarini DJ, Shah NG, Wach A, Brachat A, et al. Additional modules for versatile and economical PCR-based gene deletion and modification in *Saccharomyces cerevisiae*. *Yeast*. 1998; 14: 953–961. [https://doi.org/10.1002/\(SICI\)1097-0061\(199807\)14:10<953::AID-YEA293>3.0.CO;2-U](https://doi.org/10.1002/(SICI)1097-0061(199807)14:10<953::AID-YEA293>3.0.CO;2-U) PMID: 9717241
46. Kubota T, Hiraga S, Yamada K, Lamond AI, Donaldson AD. Quantitative proteomic analysis of chromatin reveals that Ctf18 acts in the DNA replication checkpoint. *Mol Cell Proteomics*. 2011; 10: M110.005561. <https://doi.org/10.1074/mcp.M110.005561> PMID: 21505101
47. Eaton ML, Galani K, Kang S, Bell SP, MacAlpine DM. Conserved nucleosome positioning defines replication origins. *Genes Dev*. 2010; 24: 748–753. <https://doi.org/10.1101/gad.1913210> PMID: 20351051